Chemical Physics 156 (1991) 251–260
North-Holland

The trans-stilbene–Ar van der Waals complex. Vibrationally averaged substitution structure in its S_0 and S_1 electronic states

B.B. Champagne, D.F. Plusquellic, J.F. Pfanstiel, D.W. Pratt
Department of Chemistry, University of Pittsburgh, Pittsburgh, PA 15260, USA

W.M. van Herpen and W.L. Meerts
Department of Molecular and Laser Physics, University of Nijmegen, 6525 ED Nijmegen, The Netherlands

Received 11 February 1991

Argon atom substitution coordinates, accurate to ± 0.02 Å, in the S_0 and S_1 states of the trans-stilbene–Ar van der Waals complex have been determined by comparing the inertial constants obtained from fits of two bands in the rotationally resolved electronic spectrum of the complex with those obtained from fits of the corresponding spectrum of the bare molecule (Champagne et al., J. Phys. Chem. 94 (1990) 6). The argon atom is found to be localized above (or below) the plane of one of the aromatic rings by ~ 3 Å in both electronic states but is displaced off the ring center by more than ~ 1 Å in both transverse directions. This geometry is not the one predicted by simple atom–atom pair potentials. Model calculations suggest that this is a consequence of the vibrational averaging that occurs on the S_0 and S_1 surfaces, and that these surfaces are significantly influenced by the anisotropy of the van der Waals interaction potential, in both electronic states.

1. Introduction

High-resolution spectroscopic measurements on van der Waals complexes provide a unique view of large amplitude motions and the anisotropy of intermolecular forces, especially in the vicinity of shallow potential minima. The most detailed information obtained to date comes from rotationally resolved microwave and IR spectra of the ground electronic states of small molecules to which rare gas atoms have been attached [1]. Rare-gas van der Waals complexes of a few prototypical large molecules in both their ground and excited electronic states also have been studied using rotationally resolved visible and UV spectroscopy [2–4].

One large molecule that readily forms van der Waals complexes is trans-1,2-diphenylethylene, or trans-stilbene (tS). Two prominent vibronic bands appear ≈ 40 and 63 cm^{-1} to the red of the O_0^0 band in the $S_1 \leftarrow S_0$ UV fluorescence excitation spectrum (FES) of tS seeded in supersonic free jets of argon. First observed by Zwier et al. [5], these bands have been assigned by Bahatt et al. [6] to the "single-atom" trans-stilbene–Ar (tSA) van der Waals complex using mass-resolved R2PI techniques. Further studies of tSA that revealed interesting dynamical behaviors of this and other tS complexes have been reported by De Haan et al. [7] and Baskin and Zewail [8].

This report describes an analysis of the two previously observed bands of tSA at full rotational resolution [9]. This analysis yields values of the center-of-mass coordinates of the argon atom (in the principal axis frame of tS) in the four vibronic levels accessed in the experiments. In all cases, the argon atom is found to be localized above (or below) the plane of one of the aromatic rings, but is significantly displaced off the ring center in both transverse directions. Model calculations of the S_0 and S_1 surfaces, also reported herein, show that these displacements cannot be reproduced by simple atom–atom pair potentials. We suggest that the inadequacy of such potentials owes its origin to the significant vibrational averaging that occurs on both surfaces, and that this

averaging is a sensitive function of the anisotropy in the van der Waals interaction potential.

2. Experimental

The experiments were carried out with the high-resolution molecular beam laser spectrometers in Nijmegen and Pittsburgh [10,11]. The molecular beam was formed by expansion of a mixture of tS vapor (Aldrich, heated to 400 K) and Ar carrier gas (at 0.25 to 1 bar) through a heated 100-μm quartz nozzle, collimated with two (Nijmegen) or one (Pittsburgh) skimmers, and crossed 30 cm (Nijmegen) or 10 cm (Pittsburgh) downstream by a tunable cw laser operating in the ultraviolet. Typically, ~600 μW of UV power was employed, the laser frequency width is less than 1 MHz. Molecular emission from the interaction zone was collected by spatially selective optics, imaged on a phototube, and detected by using photon counting techniques. In Pittsburgh, the FES, I_2 absorption spectrum, etalon markers, and laser power curve were recorded simultaneously with an on-line data acquisition system, providing calibrated and normalized data that are accurate to ±0.1 MHz in relative frequency and ±100 MHz in absolute frequency. Model potential calculations were performed on an FPS-500 vector processor machine.

3. Results and analysis

Representative results for the two vibronic bands, tSA-63 and tSA-40, are shown in figs. 1 and 2, respectively. Both figures are divided into three panels that illustrate three successive horizontal scale expansions of the data and the corresponding computer simulations. The top panels show the full experimental contours of tSA-63 and tSA-40 and span ≈1 cm^{-1} and 0.6 cm^{-1}, respectively. Despite the very dense rotational features, both bands exhibit the clearly defined P-, Q-, and R-branch structure that is characteristic of parallel-type selection rules. The middle panels of both figures expand the indicated portions to an intermediate frequency scale. The bottom panel of fig. 1, which spans ≈1000 MHz, shows details of the R-branch structure of tSA-63 at full experimental resolution. The bottom panel of fig. 2, which spans

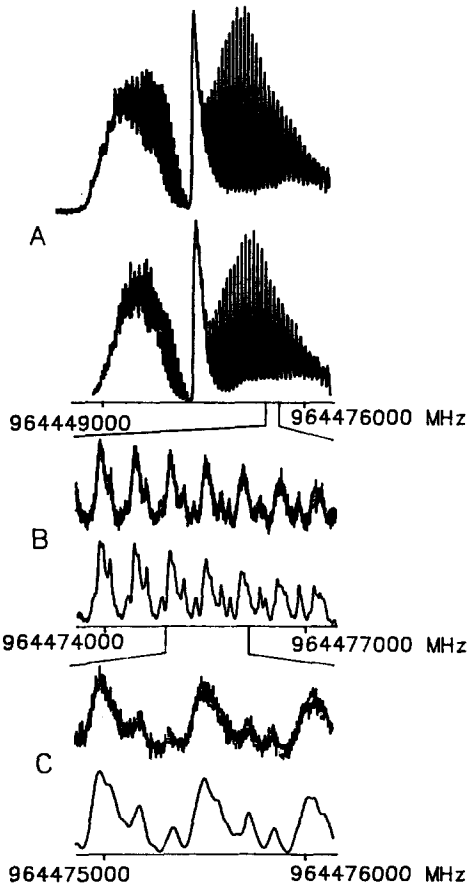

Fig. 1. The rotationally resolved fluorescence excitation spectrum of the O_0^0 band of the $S_1 \leftarrow S_0$ transition of trans-stilbene–Ar, 63 cm^{-1} to the red of the O_0^0 band of trans-stilbene (at 32234.7 cm^{-1}). Panel A shows the overall experimental band contour (top) spanning ~1 cm^{-1} and the corresponding computer simulation (bottom). Panel B shows a portion of the R-branch of the experimental spectrum (top) and the corresponding computer simulation (bottom) at intermediate resolution. Panel C shows a small section of the R-branch at full experimental resolution (top) and the corresponding computer simulation (bottom). All simulations assume a rotational temperature of 7 K. The prominent bright center portions of the contours (at their characteristic "2B" parallel band separation) are due to unresolved $K_{-1}=0$, 1, 2, 3, 4 lines progressing to the blue as $\sim K_{-1}^2(\Delta A - \Delta B_{av})$. The dimmer contours in between the brighter central portions are due mostly to asymmetry split $K_{-1}=1$, 2, 3 lines.

≈3000 MHz, shows portions of the Q- and R-branches of tSA-40. Both full contour traces were simulated using more than 5000 calculated lines, with

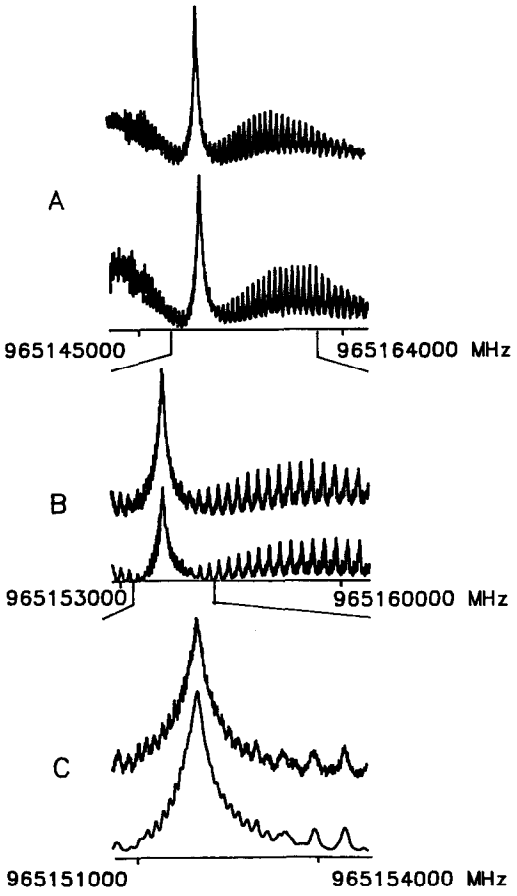

Fig. 2. The rotationally resolved fluorescence excitation spectrum of the O_0^0+23 cm^{-1} band of the $S_1 \leftarrow S_0$ transition of trans-stilbene–Ar, 40 cm^{-1} to the red of the O_0^0 band of trans-stilbene. Panel A shows the overall experimental band contour (top) and the corresponding computer simulation (bottom). Panel A spans ~0.6 cm^{-1}. Panel B shows a portion of the experimental spectrum (top) that includes contributions from P-, Q-, and R-branch transitions and the corresponding computer simulation (bottom) at intermediate resolution. Panel C shows a small section of the Q- and R-branches (top) and the corresponding computer simulation (bottom). All simulations assume a rotational temperature of 7 K. The dominant features in panel C are a clear progression to the red of subbands of a given K_{-1}, quantum number and a progression to the blue of Q-subbranches of a given K_{-1} quantum number.

a Lorentzian linewidth (fwhm) of 70 ± 10 MHz. This width is identical to that found in the rotationally resolved FES of the O_0^0 band of the bare, uncomplexed tS [12]. Therefore, we conclude that the presence of a single, weakly bound argon atom does not substantially affect the lifetime of tS in the zero-point vibrational level (ZVL) of its S_1 electronic state.

The rotational analysis was performed using an expanded version of the program ASYROT [13] that has been integrated with sophisticated computer graphics. Fits of both spectra were made by working simultaneously with portions of the experimental spectrum, the simulated contours, and the deconvoluted "stick" spectrum. Tentative spectral assignments were made based on a guessed set of rotational parameters; these parameters were then optimized with least squares [14] statistical analysis software. Convergence was deemed sufficient when the new least squares optimized parameters were equal to previously determined parameters to within the statistical uncertainty of the fit. The analysis of tSA-63 utilized 513 experimental line frequencies and converged to a standard deviation of 8.0 MHz. The analysis of tSA-40 utilized 402 lines and converged to a standard deviation of 10.2 MHz. We employed Watson's distortable asymmetric rotor Hamiltonian [15] in both fits. However, we found that only "rigid-rotor" terms were necessary for good convergence of the fits. Inclusion of higher-order distortion terms revealed that they were ill-determined by the experimental data. At least 98% of the experimentally observed intensity can be accounted for by assuming *a*-axis selection rules and rotational temperatures of order 7 K.

The parameters derived from fits of the experimental spectra of tSA are summarized in table 1. Included for comparison are the corresponding parameters derived from the fit of the O_0^0 band of tS itself [12]. Like the ZVL's of the S_0 and S_1 states of the bare molecule, the vibrational levels examined in the $S_1 \leftarrow S_0$ spectrum of the complex are rigid, near prolate asymmetric tops. However, the rotational constants of the complex are very different from those of tS. The largest change observed is in the A'' values which decrease by more than 60%. The percentage decreases in B'' and C'' are much smaller, of order 20%. Additionally, the complex levels exhibit very large (negative) inertial defects compared to the bare molecule levels. Finally, we note that the changes in A, B, and C ($\Delta A = A' - A''$, etc.) that occur on excitation of the complex to its S_1 state are very small, 5.8 MHz or less. In contrast, tS exhibits a ΔA value of -71.1 MHz. (The values of $(B'+C')/2 = B'_{av}$

Table 1
Inertial parameters and band origins derived from fits of two rotationally resolved vibronic bands in the $S_1 \leftarrow S_0$ spectrum of the tS–Ar van der Waals complex and of the O_0^0 band of uncomplexed tS

State	Constant	tSA-63 [a]	tSA-40 [a]	tS [a,b]
S_0	A''	1033.6±4.7	1042.3±19.6	2611.3±7.7 MHz
	B''	212.4±0.1	212.3±0.1	262.9±0.1 MHz
	C''	195.3±0.1	195.7±0.1	240.6±0.1 MHz
	κ''	−0.9592	−0.9608	−0.9812
	$\Delta I''$ [c]	−280.4±0.1	−282.9±9.2	−15.3±0.6 amu Å^2
S_1	ΔA	5.84±0.06	−4.7±0.2	−71.14 ±0.06 MHz
	ΔB	1.925±0.008	2.94±0.02	5.928±0.004 MHz
	ΔC	4.180±0.006	4.38±0.02	3.963±0.005 MHz
	$\Delta\kappa$	−0.0055	−0.0030	0.0023
	$\Delta(\Delta I)$ [c]	−30.1±0.1	−26.2±0.4	2.9±0.9 amu Å^2
	Band origin [d]	32170.986	32194.006	32234.744 cm^{-1}

[a] Error bars for the A'', ΔA, ΔB, and ΔC rotational constants are the square roots of the variances obtained from the least squares analysis. The B'' and C'' rotational constants obtained from the least-squares analysis are 212.38, 212.35, 262.86 and 195.27, 195.66, 240.56 MHz, respectively. However the precision of these values is reduced to ±0.1 MHz by possible systematic errors in the experiment (ref. [11]).
[b] Ref. [12]. [c] Inertial defects, $\Delta I = I_c - I_b - I_a$. [d] ±0.002 cm^{-1}.

computed from our data for the complex, 206.9 and 207.6±0.1 MHz for tSA-63 and tSA-40, are in good agreement with the less precise B'_{av} values determined for the complex from recent quantum beat studies, 207±4 and 209±6 MHz, respectively [8].)

Despite the relatively small differences in the absolute values of the rotational constants derived from tSA-63 and tSA-40, the bands are quite different in appearance. The spectroscopy that gives rise to these differences is quite easy to understand. In the prolate symmetric top limit one can consider the bands as being composed of K ($\equiv K_{-1}$) quantum number subbands that resemble textbook diatomic molecule rotational spectra with clearly defined P-, Q-, and R-branches [16]. How these K subbands are shifted with respect to one another depends largely on $\Delta K^2 = (\Delta A - \Delta B_{av})K^2$. tSA-63 has a small positive Δ that produces a progression towards the blue of the P-, Q-, and R-branches. tSA-40, on the other hand, has a small negative Δ that produces a progression towards the red of these branches. The appearance of the Q-branch is additionally dependent on ΔB and ΔC. Q-branches of a given K progress linearly in J with these values. ΔB and ΔC are both positive, in both tSA-63 and tSA-40, producing blue shifts of successive J lines. Thus, since the two shifts are in the same direction in tSA-63, but in opposite directions in tSA-40, the Q-branch in the former is degraded towards the blue but the Q-branch in the latter is nearly symmetric.

4. Structure of the complex

Our goal now is to use the information gained from the measurements on tS and tSA to establish the structure of the complex, first in its electronic ground state. We assume, for the moment, that the complex contains one Ar atom, as suggested by the earlier R2PI result [6]. t-Stilbene itself is a planar molecule in the ZVL of S_0, with the center of mass located equidistant between the two ethylenic carbons. The a inertial axis lies in the plane and passes through the two ring centers; the b and c inertial axes are, respectively, in-plane and out-of-plane, as shown below (scheme 1)

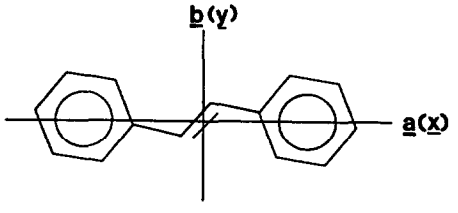

Scheme 1.

Now, of course, we do not know where the corresponding axes of the complex lie, a priori, since the Ar may attach itself at any one (or more) of several different possible positions. But consideration of the changes in the ground state rotational constants and inertial defects that occur on complexation, together with the observations that the $S_1 \leftarrow S_0$ transitions of both tS and tSA are predominantly *a*-axis polarized, strongly suggests that there *is* a preferred binding site, and that this site is above (or below) one of the benzene rings. A similar conclusion was reached by Baskin and Zewail [8]. Parenthetically, we note here that since the independently determined ground state rotational constants of the two complex bands are the same, within experimental error, the two bands must originate in the same vibrational level, presumably the ZVL of S_0 tSA.

One further assumption, that the equilibrium geometry of the tS framework is unchanged on complex formation, makes possible a quantitative determination of the coordinates of the Ar atom in the tS inertial frame. We treat the problem within the framework of Kraitchman's equations [17], so powerfully utilized in microwave spectroscopy and recently extended to optical spectroscopy by this group [3,18, 19]. The conventional application of these equations utilizes the changes in moments of inertia resulting from single (or multiple) isotopic substitution(s) of an atom to determine its principal axis coordinates. But a careful study of the classical mechanics underlying these equations reveals that *any* mass effect that results in a movement of the principal frame can be used to determine the position of the affected mass, whether substituted *or* added. The key assumption is that the substitution, *or* addition, does not change the positional relationships of the mass centers that make up the original inertial frame. Thus, by comparing the moments of inertia of the complex with those of the bare molecule using Kraitchman's equations, we can determine the position of the attached atom (or group) in a van der Waals complex providing that the substrate structure does not change. Structures derived using this method are called "substitution structures" [17].

Subject to the same assumption, the method described above should apply equally well to both states accessed in the electronic transition. It is not necessary that the inertial axes of the two states be the same. However, there is no evidence from the spectra for any reorientation of these axes on $S_1 \leftarrow S_0$ excitation, in either the bare molecule or the complex.

The Ar coordinates that result from applications of Kraitchman's equations to both the ground and excited electronic states of tSA-63 and tSA-40 are reported in table 2. The results for the ground states, which are the same within experimental error, also are plotted in fig. 3. Owing to the r^2 dependence of moments of inertia, there is an inherent sign ambiguity in all of the coordinates x, y and z (parallel to a, b, and c, respectively), resulting in eight possible Ar atom positions. However, there are only two unique ones, depending only on the sign of y, since $\pm x$ and $\pm z$ are symmetry-related coordinates in tS itself. Fig. 3 shows, unambiguously, that the Ar atom in tSA is localized over one of the benzene rings, is

Table 2
Center-of-mass coordinates, in the principal axis frame of tS, of the Ar atom in the vibronic levels accessed in two $S_1 \leftarrow S_0$ bands of the tSA van der Waals complex [a)]

State	Coordinate (Å)	tSA-63	tSA-40
S_0	$\|x\|$	2.89±0.01	2.90±0.03
	$\|y\|$	1.23±0.02	1.20±0.05
	$\|z\|$	3.01±0.02	3.00±0.07
	$\|R\|$	4.35±0.01	4.34±0.02
S_1	$\|x\|$	2.91±0.01	2.88±0.03
	$\|y\|$	1.01±0.02	1.02±0.05
	$\|z\|$	3.05±0.02	3.04±0.07
	$\|R\|$	4.34±0.01	4.31±0.02

[a)] Error estimates in the coordinates were determined by propagating the experimental errors in the rotational constants through Kraitchman's equations.

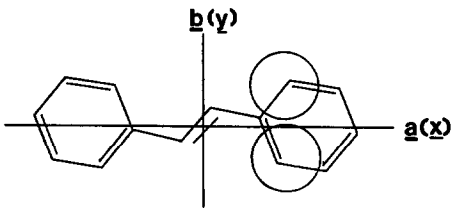

Fig. 3. Geometry of the trans-stilbene–Ar van der Waals complex. Two possible positions of the attached argon, in the S_0 electronic state, are shown as open circles.

displaced away from the ring center by more than 1 Å in both transverse directions, and sits above (or below) the ring plane by 3.01 Å. Electronic excitation of either vibronic band of the complex produces very little change in this position. The only statistically significant change in the derived values of $|x|$, $|y|$, and $|z|$ for the two S_1 levels, tSA-63 and tSA-40, is along the y-coordinate. $|y|$ decreases by ~ 0.2 Å in both cases. We conclude that the Ar atom is relatively insensitive to changes in the electronic distribution that occur on $S_1 \leftarrow S_0$ excitation of tS, at least for the vibronic levels we have probed.

The changes in the A rotational constants on $S_1 \leftarrow S_0$ excitation are significantly smaller in both tSA-63 and tSA-40 than in tS. The large change in A for tS seems to be dominated by ~ 0.01 Å increases in aromatic C–C bond distances perpendicular to the a rotational axis of tS that significantly reduce the A' rotational constant [12]. In tSA, even though these aromatic C–C bonds are probably still similarly affected by electronic excitation, there is an offsetting decrease of ~ 0.2 Å in the $|y|$-coordinate of the Ar atom that increases the A' value of the S_1 state. The two effects apparently cancel in tSA, producing small ΔA values.

The assumptions made in the above structure determination can be tested in the following way. Shown in table 3 is a comparison of the experimental rotational constants of tSA-63 and tSA-40 with those for tS itself, and with a set of theoretical constants for all vibronic levels of tS and tSA examined to date by high-resolution methods. The theoretical constants for the bare molecule in both S_0 and S_1 were calculated from the QCFF/PI geometries determined by Negri et al. [20]. The agreement between theory and experiment is remarkably good, for both states, lending credence to the claim that the equilibrium structure of tS is planar in both ZVL's. The theoretical constants for the complex were calculated for a structure constructed by adding a single Ar atom to the unperturbed tS, frozen in its QCFF/PI configuration, with the coordinates for the Ar atom being those determined by experiment. Comparison of the experimental rotational constants of the complex with those computed in this way shows (cf. table 3) that the two sets of values are in excellent agreement, in most cases even better than that for tS itself. This confirms that tSA-63 and tSA-40 are both $S_1 \leftarrow S_0$ vibronic bands of a single atom complex. Additionally, the calculation confirms that the key assumption made in our treatment of this problem, that the structure of the substrate is unaffected by complex formation, is a good one.

Adding an Ar atom to tS rotates and displaces the inertial frame towards the attached atom. A typical rotation matrix that describes how the substituted frame $(a'b'c')$ is related to the unsubstituted frame (abc) is shown below,

$$\begin{pmatrix} a' \\ b' \\ c' \end{pmatrix} = \begin{pmatrix} -0.987 & -0.066 & -0.149 \\ 0.157 & -0.642 & -0.750 \\ -0.046 & -0.763 & 0.645 \end{pmatrix} \begin{pmatrix} a \\ b \\ c \end{pmatrix}. \quad (1)$$

From this result, we see that the new inertial axes

Table 3
Comparison of experimental and theoretical rotational constants (in MHz) of tS and tSA in their ground and excited states [a]

Rotational constant	tSA/S_0(−63)	tSA/S_0(−40)	tS/S_0	tSA/S_1(−63)	tSA/S_1(−40)	tS/S_1
A, expt	1034	1042	2611	1039	1038	2540
A, theory	1039	1048	2659	1046	1044	2598
A(t)−A(e)	+0.48%	+0.58%	+1.8%	+0.67%	+0.58%	+2.3%
B, expt	212	212	263	214	215	269
B, theory	211	211	262	211	212	264
B(t)−B(e)	−0.47%	−0.47%	−0.38%	−1.4%	−1.4%	−1.9%
C, expt	195	196	241	199	200	245
C, theory	194	194	238	197	197	240
C(t)−C(e)	−0.51%	−1.0%	−1.2%	−1.0%	−1.5%	−2.0%
ΔI, expt amu Å^2	−280.4	−282.9	−15.3	−310.5	−309.1	−12.4
ΔI, theory amu Å^2	−278.9	−281.6	0	−308.5	−307.2	0

[a] See text for a description of the methods used to obtain the theoretical constants.

make substantial angles with the old ones. Consequently, the rotational constants of the complex are much more sensitive to out-of-plane distortions of the tS frame. Thus, our earlier conclusion that the bare molecule is planar in both electronic states is made firmer by the results in table 3. If a significant nonplanarity existed in the tS frame, the agreement between calculated and observed rotational constants of the complex would be poorer than that for the bare molecule alone. This is not the case, for either electronic state. Additionally, we predict from the above result that the $S_1 \leftarrow S_0$ transition of the complex should exhibit hybrid character. If the transition moment remains parallel to the a inertial axis of the substrate, it will make an angle of $\sim 9°$ with a', introducing a small amount of perpendicular character into the O_0^0 band of the complex. We have not detected this in our spectra, which is the expected result given their complexity and the direct-cosine-squared dependence of band character.

Argon atom coordinates have been measured for several other van der Waals complexes of large molecules from their rotationally resolved spectra. It is particularly interesting to compare the derived values of the out-of-plane z-coordinate in cases where the Ar is attached to a planar, or near planar frame. In the S_1 states of tetrazine-Ar, fluorene-Ar, and benzene-Ar, these are $|z| = 3.44$ [2], 3.46 [3], and 3.58 Å [4], respectively. In pyrrole-Ar, the ground state has been examined by microwave spectroscopy, yielding $|z| = 3.55$ Å [21]. All of these values are larger than that measured for tSA, $|z| = 3.01$ Å.

3. Modeling the tSA potential surface

The nuclear framework of a molecule is not rigid because the atoms undergo vibrational motions about their equilibrium positions simultaneously with rotation. As internuclear distances and angles change when the molecule vibrates, moments of inertia and the atomic positions derived from them depend in a complicated way on the nature of these vibrations. Zero-point vibrational effects tend to cancel in the calculation of atomic positions with Kraitchman's equations [17]. Nonetheless, we can easily imagine, especially for a weakly bound atom like Ar in tSA, that its ZVL substitution coordinates might still be influenced by large amplitude intermolecular vibrational motions, perhaps to a significant degree. These vibrational motions, in turn, are governed by a tS-Ar potential energy function. Here, we attempt to gain information about that function in both electronic states from the measured Ar atom coordinates.

Our approach is not new. Like others [3,8,22,23], we construct the tS–Ar potential as a superposition of pairwise additive atom–atom potentials

$$V(R) = \sum_i v_i |R - r_i| \,, \tag{2}$$

where

$$v_i(r_i) = 4\epsilon_i \left[\left(\frac{\sigma_i}{r_i} \right)^{12} - \left(\frac{\sigma_i}{r_i} \right)^{6} \right]. \tag{3}$$

Here R is a vector from the tS COM to the Ar atom, the r_i's are the positions of the atoms in tS relative to its COM, and the ϵ_i, σ_i are the usual Lennard-Jones parameters. (Initial values of these parameters were taken from Ondrechen et al. [22] and are listed in table 4, together with subsequent values used in more refined calculations.) We then express the kinetic energy of the attached Ar in the inertial coordinate system of tS, using the reduced mass of the complex,

$$T = \frac{(\hat{P}_a^2 + \hat{P}_b^2 + \hat{P}_c^2)}{2\mu}, \quad \mu = \frac{M_{\mathrm{Ar}} M_{\mathrm{tS}}}{M_{\mathrm{Ar}} + M_{\mathrm{tS}}}, \tag{4}$$

and add these terms to eq. (2) to form the model Hamiltonian. We thus neglect the angular momentum, and the related kinetic energy, associated with rotation of the tS frame relative to Ar, an assumption

Table 4
Potential energy parameters used in the model calculations

Calculation	Atom pair	$\epsilon(\mathrm{cm}^{-1})$	σ(Å)
I [a]	Ar–C_e	40.2	3.42
	Ar–C_{ph}	40.2	3.42
	Ar–H	33.0	3.21
II	Ar–C_e	40.2	3.42
	Ar–C_{ph}	40.2	3.08
	Ar–H	33.0	3.21
III	Ar–C_e	40.2	3.42
	Ar–$C_{ph}(p)$	40.2	3.08
	Ar–$C_{ph}(o, m)$	40.2	2.57
	Ar–H	33.0	3.21

[a] Parameters taken from ref. [22].

justified by the rigid rotor fits to the tSA data. The problem is thus reduced to one in which a single reduced mass moves in the potential of a bare tS molecule. Selecting a product basis of 13 particle-in-a-box wavefunctions for each coordinate, we then diagonalize the 13^3-dimensional Hamiltonian to obtain a set of eigenfunctions and eigenvalues. A point-by-point integration scheme of $V(R)$ over all 13^3 functions using a $500\times500\times500$ point grid was employed. The Rayleigh–Ritz criterion was used to optimize the size of the box, to 12 Å along a, 5 Å along b, and 5 Å along c. The vertical origin of the box was placed near the minimum of the potential. Expectation values of the Ar geometrical coordinates (squared) were then computed by summing over the appropriate eigenvector coefficients. Similar calculations using a harmonic oscillator basis gave identical results.

The results for the literature potential (calculation I) are listed in table 5. The global minimum is at -420 cm^{-1}. The quantitative agreement of the calculated Ar atom position with the experimental results for the (presumed) ZVL of S_0 tSA ($|x|=2.9$, $|y|=1.2$, $|z|=3.0$ Å) is very poor. Of particular interest is the calculated value of $|x|$, 1.1 Å, which places the Ar near the ethylenic portion of the tS molecule rather than near one of the aromatic rings.

An insight into this result is provided by fig. 4, which shows a cross section of the potential along x ($\|a$) at constant $|y|$ ($=0$) and two values of $|z|$, 3.15 Å and 3.40 Å. The generic form of the potential shows six minima. Two lie on either side of the ethylenic portion of tS, two lie over the aromatic rings, and two lie at either end of the molecule. Of these, the four inside minima are lower and roughly comparable in depth. Varying $|z|$ changes the relative heights of these minima; at $|z|=3.15$ Å, the aromatic binding sites are preferred whereas at $|z|=3.40$ Å, the ethylenic binding sites are preferred. (The one-dimensional barriers along x are typically large compared to the zero-point energy for motion of the Ar atom, so it appears proper to speak of localization along this coordinate.) Clearly, this must be because, at smaller $|z|$, the Ar can sample both portions of the surface at relatively favorable distances. Stated differently, it must be that the tS–Ar potential becomes more repulsive when the Ar approaches the ethylenic portion of the molecule at distances less than 3.4 Å than when it approaches the aromatic rings. This conclusion appears consistent with what is known about the Ar–ethylene potential [24].

We have modified the potential to model this effect. The results are reported in tables 4 and 5 (calculation II). Reducing the aromatic carbon σ's by 15% relative to those of the ethylenic carbons brings both

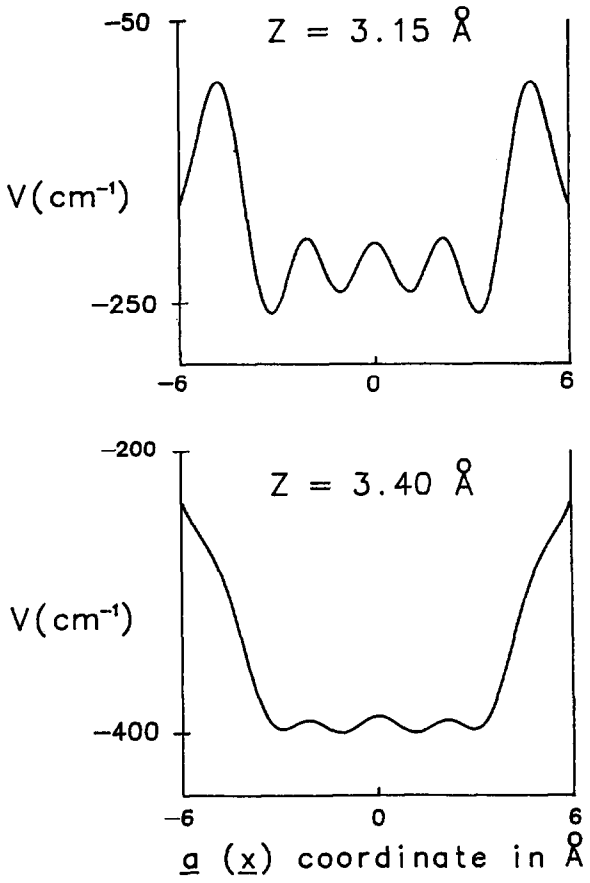

Fig. 4. Slices of the model S_0 potential energy surface along x, with $y=0$, $|z|=3.15$ Å (top), and $|z|=3.40$ Å (bottom).

Table 5
Calculated Ar atom coordinates in S_0 tSA (in Å) [a]

Calculation	$\|x\|$	$\|y\|$	$\|z\|$
I	1.1	0.7	3.5
II	3.1	0.2	3.0
III	2.8	1.0	3.3
Expt.	2.9	1.2	3.0

[a] See text for description of the calculations.

the calculated $|x|$- and $|z|$-coordinates into much better agreement with the experimental values. Additionally, the global minimum is reduced to -484 cm^{-1}.

One other dimension of the tS–Ar potential remains to be explored, that along y. The potentials employed in calculations I and II give a vibrationally averaged y-coordinate that is significantly smaller than the experimental value. In calculation I (at $|x|=1.1$ and $|z|=3.5$ Å), $V(y)$ exhibits two minima, symmetrically displaced with respect to the ethylenic portion of the molecule at $y=0$. In calculation II (at $|x|=3.1$ and $|z|=3.0$ Å), $V(y)$ exhibits three minima, also symmetrically displaced with respect to $y=0$. The center minimum, over an aromatic ring, is significantly lower in energy than the outer two minima. Calculation I gives a better value for the y-coordinate. We attribute this to the significantly smaller slope of the potential along y in calculation I. Thus, $V(R)$ must be modified in a second way in order to correctly model the experimental results. Not only is it necessary to distinguish the ethylenic and aromatic binding sites, but it is also necessary to flatten the potential along y.

We also have modified the potential to model both of these effects simultaneously. The results are reported in tables 4 and 5 (calculation III). Again, reducing the aromatic carbon σ's brings both the calculated $|x|$- and $|z|$-coordinates into better agreement with the experimental values. But a further reduction of the σ values of the *ortho* and *meta* carbons (by 25% relative to those of the ethylenic carbons) also brings the calculated $|y|$-coordinate into better agreement with experiment. The latter change gives the three minima along y approximately the same values, thus making the potential flatter along this coordinate. Clearly, the surface must be steeper along this coordinate in S_1, since $|y|$ decreases on electronic excitation. The global minimum on the S_0 surface in calculation III is -341 cm^{-1}.

The calculations also give eigenvalues for the tS–Ar intermolecular vibrational modes. Comparison of these with the experimental S_1 vibrational spacing of 23 cm^{-1} suggests that this mode is an in-plane tS–Ar bending vibration, principally along x, in agreement with the assignment of Zwier et al. [5] but in disagreement with the calculations of Bahatt et al. [6]. All of our calculations show that the first mode having significant out-of-plane character lies at 30 cm^{-1} or above in energy. But there is significant mixing between the two types of modes in tSA, giving these labels significantly less meaning than in benzene [23]. Finally, we note that the finding that there is little or no change in $|y|$ on excitation of one quantum in this mode is consistent with the character of the surface along this coordinate.

6. Summary

Summarizing, we have obtained rotationally resolved spectra of two vibronic bands in the $S_1 \leftarrow S_0$ electronic spectrum of the single atom trans-stilbene–Ar van der Waals complex. Fits of these spectra to a rigid rotor Hamiltonian yield the vibrationally averaged rotational constants and moments of inertia of the complex in both electronic states. Argon atom substitution coordinates in the complex, accurate to ± 0.02 Å, have been determined by comparing its moments to those of the bare trans-stilbene molecule. Comparison of these coordinates with those calculated using model pair potentials shows that satisfactory agreement with experiment can be obtained only if significant modifications of the accepted Ar–C Lennard-Jones parameters are made. The modifications that are found to be necessary suggest that anisotropies in the potential are quite important. Additionally, it appears that model pair potentials are too corrugated to correctly reproduce the effects of the extensive vibrational averaging that are observed in the trans-stilbene–Ar complex.

Acknowledgement

This work is dedicated to Professor Jan Kommandeur on the occasion of his 60th birthday. We are indebted to him for his enthusiastic support of our research in high-resolution spectroscopy that owes its origin to a common interest in radiationless transitions. We also thank the U.S. National Science Foundation and the Nederlandse Organisatie voor Wetenschappelijk Onderzoek for financial support, and Nick Nystrom for assistance with the calculations.

References

[1] J.M. Hutson, Ann. Rev. Phys. Chem. 41 (1990) 123.

[2] C.A. Haynam, D.V. Brumbaugh and D.H. Levy, J. Chem. Phys. 80 (1984) 2256;
For a review of more recent work, see
D.H. Levy, in: Structure and Dynamics of Weakly Bound Molecular Complexes, ed. A. Weber (Reidel, Dordrecht, 1987) p. 231.

[3] W.M. van Herpen, W.L. Meerts and A. Dymanus, J. Chem. Phys. 87 (1987) 182;
W.M. van Herpen and W.L. Meerts, Chem. Phys. Letters 147 (1988) 7.

[4] Th. Weber, A. von Bargen, E. Riedle and H.J. Neusser, J. Chem. Phys. 92 (1990) 90.

[5] T.S. Zwier, E. Carrasquillo, M. and D.H. Levy, J. Chem. Phys. 78 (1983) 5493.

[6] D. Bahatt, U. Even and J. Jortner, Chem. Phys. Letters 117 (1985) 527.

[7] D.O. DeHaan, A.L. Holton and T.S. Zwier, J. Chem. Phys. 90 (1989) 3952.

[8] J.S. Baskin and A.H. Zewail, J. Phys. Chem. 93 (1989) 5701.

[9] For a preliminary report, see
W.M. van Herpen, W.A. Majewski, D.W. Pratt and W.L. Meerts, in: Structure and Dynamics of Weakly Bound Molecular Complexes, ed. A. Weber (Reidel, Dordrecht, 1987) p. 279.

[10] W.A. Majewski and W.L. Meerts, J. Mol. Spectry. 104 (1984) 271.

[11] W.A. Majewski, D.F. Plusquellic and D.W. Pratt, J. Chem. Phys. 90 (1990) 1362.

[12] B.B. Champagne, J.F. Pfanstiel, D.F. Plusquellic, D.W. Pratt, W.M. van Herpen and W.L. Meerts, J. Phys. Chem. 94 (1990) 6.

[13] F.W. Birss and D.A. Ramsay, Comput. Phys. Commun. 38 (1984) 83.

[14] W.H. Press, B.P. Flannery, S.A. Teukolsky and W.T. Vetterling, Numerical Recipes in C (Cambridge Univ. Press, Cambridge, 1988).

[15] J.K.G. Watson, J. Chem. Phys. 46 (1967) 1935.

[16] G. Herzberg, Infrared and Raman Spectra (Van Nostrand Reinhold, New York, 1966) p. 418, for a nice illustration of these trends.

[17] W. Gordy and R.L. Cook, Microwave Molecular Spectra, 3rd Ed. (Wiley-Interscience, New York, 1984).

[18] J.R. Johnson, K.D. Jordan, D.F. Plusquellic and D.W. Pratt, J. Chem. Phys. 93 (1990) 2258.

[19] A. Held, D.F. Plusquellic, J.L. Tomer and D.W. Pratt, J. Phys. Chem. 95 (1991) 2877.

[20] F. Negri, G. Orlandi and F. Zerbetto, J. Phys. Chem. 93 (1989) 5124.

[21] R.K. Bohn, K.W. Hillig II and R.L. Kuczkowski, J. Phys. Chem. 93 (1989) 3456.

[22] M.J. Ondrechen, Z. Berkovitch-Yellin and J. Jortner, J. Am. Chem. Soc. 103 (1981) 6586.

[23] G. Brocks and T. Huygen, J. Chem. Phys. 85 (1986) 3411.

[24] S.R. Hair, J.A. Beswick and K.C. Janda, J. Chem. Phys. 89 (1988) 5970, and references therein.